THE JOURNAL OF PHYSICAL CHEMISTRY B

ARTICLE

pubs.acs.org/JPCB

Theory of Gas Hydrates: Effect of the Approximation of Rigid Water Lattice

Hrushikesh Pimpalgaonkar, Shivanand K. Veesam, and Sudeep N. Punnathanam*

Department of Chemical Engineering, Indian Institute of Science, Bangalore -560012, India

Supporting Information

ABSTRACT: One of the assumptions of the van der Waals and Platteeuw theory for gas hydrates is that the host water lattice is rigid and not distorted by the presence of guest molecules. In this work, we study the effect of this approximation on the triple-point lines of the gas hydrates. We calculate the triple-point lines of methane and ethane hydrates via Monte Carlo molecular simulations and compare the simulation results with the predictions of van der Waals and Platteeuw theory. Our study shows that even if the exact intermolecular potential between the guest molecules and water is known, the dissociation temperatures predicted by the theory are significantly higher. This has serious implications to the modeling of gas hydrate thermodynamics, and in spite of the several impressive efforts made toward obtaining an accurate description of intermolecular interactions in gas hydrates, the theory will suffer from the problem of robustness if the issue of movement of water molecules is not adequately addressed.

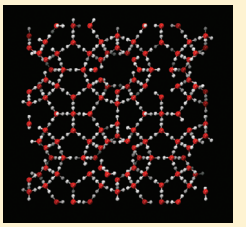

1. INTRODUCTION

Gas hydrates are crystalline inclusion compounds with the host lattice made up of water molecules and guest species consisting of low molecular weight gases such as methane, ethane, carbon dioxide, etc.[1] The host lattice is made up of water molecules connected to each other in a tetrahedral fashion via hydrogen bonds. The crystalline lattice contains regularly spaced cavities called cages, whose dimensions are molecular in scale and usually contain at most one guest molecule. Since all the cavities need not be occupied, unlike inorganic hydrates, the ratio of number of gas molecules to water molecules is not fixed, and hence they are nonstoichiometric. Over the years, there has been an increasing interest in gas hydrates due to scientific and technological reasons. In nature, gas hydrates containing primarily methane, occur in deep sea floor sediments and in permafrost regions.[1] It has been estimated that the total amount of energy available from the natural gases trapped in these hydrates exceeds that available from all the conventional fossil fuels combined.[2] Hence, they are regarded as an important future fuel resource. Formation of gas hydrates in the form of plugs can also occur in deep sea natural gas transmission pipelines leading to their blockage.[3] As a result, there are significant ongoing research efforts aimed at understanding the kinetics of hydrate formation[4−6] and developing means to prevent their formation.[2,7] Gas hydrates have been proposed as a storage medium for a variety of applications such as transportation of natural gas,[8,9] carbon dioxide sequestration,[10,11] etc. This is due to their ability to store gases in a concentrated form at moderate pressures; e.g., a unit volume of gas hydrate is able to store 180 STP of gas.[2] Natural gas hydrates also play an important role in climate change studies. Since methane is a strong greenhouse gas, any large-scale release of methane from gas hydrates present on the sea floors and permafrost regions can cause an increase in global temperatures. This in turn provides a positive feedback leading to more dissociation of methane hydrates and can cause a runaway global warming effect.[2,10,12]

To exploit the hydrates for technological and scientific use, an understanding of the properties of these materials is desired. In this context, significant efforts have been made over the past half century toward developing theories for predicting the thermodynamic properties of gas hydrates. One such theory, developed using statistical thermodynamics, was proposed by van der Waals and Platteeuw,[13] henceforth referred to as "vdWP theory". It is based on the cell theory of Lennard-Jones and Devonshire[14,15] and models the gas hydrate as a collection of individual cages containing guest molecules. The approximations built into the vdWP theory make it possible to factorize the partition function into a product of individual cell partition functions resulting in an analytical expression for the partition function. The vdWP theory and its subsequent modifications have been quite successful in describing the thermodynamic properties of gas hydrates and is widely used in the industry.[1] However, the approximations built into the vdWP theory, while making the theory computationally tractable, also lead to many problems. The parameters of the vdWP theory are obtained by regression from the monovariant three-phase equilibrium data.[1] As a result, theory has poor predictive capability outside the range of fitting. Such problems can be alleviated by improving the approximations built into the theory, thereby making it more robust. There have been several studies that have contributed to a steady improvement over the original theory since 1959. A vast majority of these have been devoted to improving the accuracy of the interactions between the guest molecule with the host lattice and other guest molecules. McCoy and Sinanoglu[16] found that the use of Kihara potential to describe the dispersion interactions between the guests and the water lattice gave improved predictions compared

Received: May 4, 2011
Revised: July 1, 2011
Published: July 05, 2011

to the Lennard-Jones 6-12 potential used in the original vdWP theory. Studies by John and Holder[17−19] and Tester and co-workers[20−24] showed that interactions of a guest molecule with water molecules beyond the first cage were significant enough to influence the phase equilibrium predictions. Recently, determination of cage potential via ab initio methods by Klauda and Sandler[25,26] and Trout and co-workers[24,27] led to more accurate predictions of hydrate phase equilibria. Other improvements over the original vdWP theory included accounting for multiple occupancy of cages,[28] inclusion of guest−guest interactions,[29] and incorporation of an increase in volume of hydrate due to occupancy of cages.[30,31] Although these modifications have helped to improve the accuracy of vdWP theory, the net result is the presence of a large number of adjustable parameters that need to be regressed from the phase equilibrium data. Due to this, there is a danger of these parameters losing their physical meaning and acting as data correlators designed to fit the experimental data.[32] Whether the vdWP theory suffers from this problem can, however, be tested only if we have an exact description of the interactions among the various species that form the gas hydrate. Since the comparison of the theory predictions with experimental data will always involve some approximation to the intermolecular interactions among the constituent molecules, one is uncertain as to whether the differences between the theory and experiments are due to failings of the theory or due to the inaccuracies in the description of the intermolecular interactions.

This situation can be alleviated by comparison of theory predictions with molecular simulation data of gas-hydrate forming systems. Since in molecular simulations, the intermolecular interactions are known exactly, such a comparison can highlight the merits or demerits of the theory itself. There have been a large number of studies on gas hydrates using molecular simulation techniques such as Monte Carlo and molecular dynamics. A few of them have studied the impact of the approximations in the vdWP theory[32−36] on the properties of gas hydrates. However, only recently, there have been studies that have determined the phase equilibrium in gas hydrate systems directly from molecular simulations.[37−39] In this paper, we have used the same techniques to compute the phase equilibria of gas hydrates formed by methane and ethane. Specifically, we compute the triple-point line denoting equilibrium between hydrate, liquid, and vapor phases and compare the simulation data with predictions of the vdWP theory. In the case of ethane hydrates, we extend our calculations to pressures below the quadruple point and compute equilibrium between hydrate, ice, and vapor phases. The major assumptions of the vdWP theory that will be addressed in this study are that (i) the host lattice is rigid and that the presence of guest molecules does not distort it, (ii) guest molecules do not interact with each other, (iii) and guest−host interaction is limited to the nearest host molecules forming the cavity. Our studies show that the approximation of considering the water lattice to be rigid leads to prediction of higher dissociation temperatures of gas hydrates. Although this approximation has been relaxed somewhat by Ballard and Sloan,[30,31] we show that it is still inadequate and accounting for movement of water molecules within the framework of the vdWP theory is necessary to make it more robust.

2. THEORY

Here, we present key equations of the vdWP theory related to our work. The equations described here follow from the discussion in Wierzchowski and Monson[36] and are applicable for gas hydrates formed by a single guest species. The starting point of the vdWP theory is the semigrand partition function for a binary mixture of water and a guest species. The final form of the semigrand partition function, Γ, for a fixed number of water molecules, N_w, in a given volume, V, at a particular temperature, T, and fugacity, f_g, of the guest is given as

$$\Gamma(N_w, V, T, f_g) = Q(N_w, V, T) \prod_i (1 + f_g C_i)^{M_i} \quad (1)$$

where Q is the canonical partition function for an empty hydrate, i.e., hydrate phase with all the cages unoccupied; C_i is the Langmuir constant for cage of type "i"; and M_i is number of cages of type "i" for every N_w water molecules. The Langmuir constant for cage of type "i" is given by

$$C_i = \frac{1}{kT} \int_{V_i} e^{-\beta u(r)} d\mathbf{r} \quad (2)$$

where k is the Boltzmann constant; V_i is the volume of the cage "i"; u is the cage potential experienced by a guest molecule due to the interaction with the host lattice; and $\beta = 1/(kT)$. In the original version of the vdWP theory, the Langmuir constants are calculated by assuming (i) the cages to be spherical and (ii) the interaction, u, to be spherically symmetric. Here, instead, we compute the exact value of the Langmuir constant via Monte Carlo integration.[21,36] From eq 1, we can obtain the fractional occupancy, Θ, of the cages as

$$\Theta = \frac{1}{M} \sum_i \frac{M_i f_g C_i}{1 + f_g C_i} \quad (3)$$

where $M = \sum_i M_i$ is the total number of cages for every N_w water molecules. One can also obtain the fugacity of water, f_w^H, in the hydrate phase by differentiating eq 1 with respect to N_w. The fugacity is then given by

$$\ln(f_w^H) = \ln(f_w^0) - \sum_i \nu_i \ln(1 + f_g C_i) \quad (4)$$

where f_w^0 is the fugacity of water in the empty hydrate at the same temperature and pressure and $\nu_i = M_i/N_w$ denotes the number of cages of type "i" per water molecule.

The crystal structure of the gas hydrate depends on the nature of the guest molecule.[1] In this paper, we study gas hydrates formed by methane and ethane which are known to exist in sI form.[1] The sI hydrate contains two types of cages, namely, the smaller dodecahedron and the larger tetrakaidecahedron. The unit cell of the sI hydrate is made up of 46 water molecules having two cages of dodecahedron and six cages of tetrakaidecahedron. Denoting these cages by subscripts "S" and "L", respectively, we can rewrite eq 3 and eq 4 as

$$\Theta = \frac{1}{M} \left(\frac{M_L f_g C_L}{1 + f_g C_L} + \frac{M_S f_g C_S}{1 + f_g C_S} \right) \quad (5)$$

$$\ln(f_w^H) = \ln(f_w^0) - \nu_L \ln(1 + f_g C_L) - \nu_S \ln(1 + f_g C_S) \quad (6)$$

respectively. In the original version of the vdWP theory, the Langmuir constant was calculated by considering only the interactions of the guest molecules with the nearest water molecules that form the cage. Subsequent workers have included contributions from all the water molecules.[17−24,30,31] The

contribution of the guest−guest interactions can be included using the mean-field approximation.[26,29] This modifies eq 5 and eq 6 as

$$\Theta = \frac{M_L f_g \exp(-\beta\Theta a_L) C_L}{1 + f_g \exp(-\beta\Theta a_L) C_L} + \frac{M_S f_g \exp(-\beta\Theta a_S) C_S}{1 + f_g \exp(-\beta\Theta a_S) C_S} \quad (7)$$

$$\ln(f_w^H) = \ln(f_w^0) - \nu_L \ln[1 + f_g \exp(-\beta\Theta a_L) C_L] - \nu_S \ln[1 + f_g \exp(-\beta\Theta a_S) C_S] \quad (8)$$

where a_L and a_S are the interaction energies of hydrocarbon molecules at the centers of the large and small cages, respectively, with the neighboring hydrocarbon molecules. Equation 7 is implicit in Θ and needs to be solved by iteration.

3. MOLECULAR MODEL

The hydrocarbon interactions, i.e., methane−methane and ethane−ethane interactions, are modeled using the united atom TRaPPE force field.[40] In this model, methane is represented by a single site, and ethane is represented as a rigid two-site dumbbell with each site representing the CH_3 group. Both methane−methane and ethane−ethane interactions consist of purely van der Waals forces between the sites and are modeled using the Lennard-Jones equation. The Lennard-Jones parameters were optimized to reproduce the experimental VLE data. Water is represented by the rigid 3-site SPC/E model.[41] This model has been used in earlier studies of hydrates and is computationally less expensive than 4 or 5 site models of water. The three sites correspond to oxygen and two hydrogen atoms. Each site is associated with a partial charge with the oxygen atom having a negative charge and the hydrogen atoms carrying positive charges. The net charge on each water molecule is zero. The intermolecular interactions are governed by Coulomb's law. In addition, the oxygen atoms also interact with each other via van der Waals forces modeled by the Lennard-Jones equation. The hydrocarbon−water interactions consist of only van der Waals forces and are modeled by Lennard-Jones equations across the various sites. The parameters for these cross interactions are obtained by application of Lorentz−Berthelot rules.

4. METHODOLOGY

In this study, we use the method of Monte Carlo molecular simulations to calculate the triple-point lines in gas hydrate systems. The triple-point lines denote the phase equilibria between liquid (or ice), vapor, and hydrate phases. The criteria for equilibrium between the three phases are equalities of temperature, T, pressure, P, and fugacities, f, of water and hydrocarbon across the three phases, i.e.

$$T^v = T^l = T^H \quad (9)$$

$$P^v = P^l = P^H \quad (10)$$

$$f_w^v = f_w^l = f_w^H \quad (11)$$

$$f_g^v = f_g^l = f_g^H \quad (12)$$

The superscripts l, v, and H represent the liquid, vapor, and hydrate phase, respectively, and the subscripts w and g represent water and the hydrocarbon molecule, respectively. Similar to previous studies of water−hydrocarbon mixtures,[38,42] we observed that the mutual solubilities of water and hydrocarbon in each other were very low. Hence, we assume the liquid and vapor phases to be composed of pure water and pure hydrocarbon, respectively. This reduces eqs 11 and 12 to

$$f_w^l = f_w^H \quad (13)$$

$$f_g^v = f_g^H \quad (14)$$

respectively. The triple point can be calculated by solving eq 9, eq 10, eq 13, and eq 14 in conjunction with the equations of state for the three phases. A similar procedure is followed for obtaining the triple points between ice, hydrate, and vapor phases. The procedure for obtaining the equations of state from molecular simulations is described below.

4.1. Equation of State of Liquid Water. The equation of state of liquid water, obtained after integrating the Gibbs−Duhem equation, is given as

$$\ln\left(\frac{f_w^l}{f_{w,0}^l}\right) = -\int_{T_0}^{T}\left(\frac{H_R^l}{RT^2}\right)_P dT + \int_{P_0}^{P}\left(\frac{V^l}{RT}\right)_{T_0} dP \quad (15)$$

where R is the universal gas constant; V^l is the specific molar volume of the liquid phase; H_R^l is the residual molar enthalpy of the liquid; T_0 is the reference temperature; P_0 is the reference pressure; and $f_{w,0}^l$ is the fugacity of water in the liquid phase at T_0 and P_0. The equation of state was obtained in two steps. In the first step, extensive simulations of liquid water in the isothermal−isobaric (N, P, T) ensemble were performed to compute the values of H_R^l and V^l. The isothermal−isobaric simulations were performed over a system size of at least 350 water molecules. Each simulation consisted of an equilibration period of 100 000 cycles followed by a production run of at least 100 000 cycles. The simulations were performed at temperatures ranging from 200 to 300 K and pressures ranging from 1 to 2000 bar. However, it was found that the fluctuations of the quantities calculated via simulations, i.e., H_R^l and V^l, especially at lower pressures, were larger than the variations of the averages with temperature and pressure. Hence, to maintain thermodynamic consistency, both H_R^l and V^l were expressed as polynomials of both T and P. The coefficients of the polynomials were obtained by linear regression and were also made to satisfy the Maxwell's rule, i.e.

$$-\left(\frac{\partial H_R^l/RT^2}{\partial P}\right)_T = \left(\frac{\partial V^l/RT}{\partial T}\right)_P \quad (16)$$

The details regarding the form of polynomials are given in the Supporting Information. The second step involved computation of the fugacity at the reference state. This was carried out by using the Hamiltonian-integration method described in Vega et al.[43] These simulations were performed in the canonical ensemble at a temperature of 215 K and density of 1010.76 kg/m^3. Each simulation consisted of 100 000 equilibration and 100 000 production cycles.

4.2. Equation of State of Ice-Ih and Empty Hydrate. The equations of state for Ice-Ih and empty sI-hydrate were obtained by methods similar to that for liquid water, as explained in

Section 4.1. Similar to liquid water, extensive simulations in the isothermal−isobaric (N,P,T) ensemble gave us values of H_R and V. Each simulation consisted of at least 100 000 equilibration cycles and 100 000 production cycles. The system size for the ice phase was 288 molecules (equivalent to 36 unit cells) and for the hydrate phase was 368 molecules (equivalent to 8 unit cells). The initial coordinates of water molecules for both the hydrate phase and the ice phase were obtained through simulated annealing, starting from a temperature of 400 K and going down to 0.1 K. Simulations of Ice-Ih were performed for temperatures ranging from 190 to 230 K and for pressures ranging from 0.1 to 2000 bar. Simulations of the empty sI hydrate were performed for temperatures between 190 and 300 K and for pressures between 0.1 and 2000 bar. H_R and V were fitted to polynomials of T and P whose coefficients were obtained by linear regression under the constraint of the Maxwell's rule [eq 16]. This ensured thermodynamic consistency upon integration of H_R and V to obtain the equations of state. The details of the curve fitting to obtain the equation of state are given in the Supporting Information. Calculation of reference state fugacity of water in the Ice-Ih and empty hydrate phases was performed using the Frenkel−Ladd method.[44,45] The details of the Frenkel−Ladd method applied to gas hydrates are given elsewhere.[36] The values of the translational (λ_T/k) and rotational (λ_R/k) parts of the spring constants for the Einstein crystal were 4.83×10^6 K/Å^2 and 4.83×10^6 K, respectively. Each simulation in the Frenkel−Ladd method consisted of 10 000 equilibration and 50 000 production cycles. The thermodynamic integration in the Frenkel−Ladd method was carried out using a 20-point Gauss−Legendre quadrature. The Frenkel−Ladd simulations for Ice-Ih were performed at a temperature of 190 K and a density of 952.858 kg/m^3, and those for the empty sI-hydrate were done at a temperature of 230 K and a density of 833.639 kg/m^3.

4.3. Equation of State of Vapor. Since methane is modeled using a single site Lennard-Jones potential, we use the 32-parameter equation of state proposed by Johnson et al.[46] For ethane, the equation of state is obtained by thermodynamic integration similar to eq 15. However, the curve fitting of H_R and V as functions of T and P, respectively, were done independently. Due to high accuracy of the data from vapor-phase simulations, the thermodynamic consistency represented by eq 16 could still be maintained. The free energy of ethane at the reference state could be obtained by integrating from the low density ideal-gas state as follows.

$$\frac{A^{ex}}{RT} = \int_0^{\rho} \left(\frac{Z-1}{\rho}\right) d\rho \tag{17}$$

where A^{ex} is the excess Helmholtz free energy; ρ is the density of the vapor; and Z is the compressibility of the vapor phase.

4.4. Equation of State of the Hydrate Phase. The hydrate phase consists of two components, namely, water and the hydrocarbon. The fugacity of water in the hydrate phase is thus a function of temperature, pressure, and the fugacity of the hydrocarbon and can be expressed as[36]

$$\ln(f_w^H) = \ln(f_w^0) - \int_0^{f_g} \frac{x_g}{x_w} \frac{df_g}{f_g} \tag{18}$$

where x_g and x_w are the mole fraction of the hydrocarbon and water in the hydrate phase, respectively. In the above equation, f_w^0 is obtained from the equation of state for the empty hydrate. In eq 18, x_g and x_w were computed by performing Monte Carlo simulations in the isothermal−isobaric semigrand (μ_g,N_w,P,T) ensemble. The procedure for computing f_w^H is detailed in Wierzchowski and Monson.[36] Thus, to obtain the fugacity of water in the hydrate phase, one has to compute the variation of x_g with f_g, i.e., the occupancy curve, in addition to the equation of state for the empty hydrate. However, instead of calculating the occupancy curves at every T and P, we follow a different strategy. We first compute the fugacity of water in the hydrate phase which is in equilibrium with the vapor phase at the reference temperature, T_0, and pressure, P_0. Using the Gibbs−Duhem equation, we can derive an expression for the variation of fugacity of water in the hydrate phase, which is in equilibrium with the vapor phase, with respect to T and P (see Appendix A). Upon integration, we obtain

$$\ln\left(\frac{f_w^H}{f_{w,0}^H}\right) = \int_{T_0}^{T} \left(\frac{H_R^H - x_g^H H_R^v}{x_w^H}\right)_P d\left(\frac{1}{RT}\right) + \int_{P_0}^{P} \left(\frac{Z^H - x_g^H Z^v}{x_w^H}\right)_{T_0} d\ln P \tag{19}$$

where $f_{w,0}^H$ is the fugacity of water in the hydrate phase at T_0 and P_0 that is in equilibrium with the vapor phase at the same T_0 and P_0. In eq 19, H_R^H, Z^H, x_g, and x_w are obtained from Monte Carlo simulations in the isothermal−isobaric semigrand (μ_g,N_w,P,T) ensemble. Each simulation was performed over 8 unit cells of the sI-hydrate and consisted of at least 10 000 equilibration and 100 000 production cycles. The hydrate phase was simulated over temperatures ranging from 190 to 300 K and pressures ranging from 0.1 to 2000 bar. The values of the fugacities of the hydrocarbon, which is required as an input to the semigrand simulations, were obtained from the equation of state of the vapor phase. H_R^v and Z^v are obtained as explained in Section 4.3.

The triple points were finally calculated by solving eqs 15 and 19 simultaneously. In addition to the above simulations, we also performed constant volume semigrand (μ_g,N_w,V,T) simulations for the hydrate phase keeping the water molecules frozen and determined the occupancy curve, i.e., variation of loading in the hydrate phase with fugacity of the vapor phase. This situation mimics the vdWP theory assumption of a frozen water lattice. The purpose of these simulations was 2-fold: one, to examine the adequacy of the mean field description for guest−guest interactions in the hydrate phase, and the other, to study the effect of rigid-water lattice approximation in the hydrate phase.

5. RESULTS AND DISCUSSION

Figure 1 shows the fractional occupancy of methane in the sI hydrate as a function of its fugacity. There are two sets of simulation data shown in the figure, one from constant pressure semigrand simulations at 20 bar and 230 K and the other from constant volume semigrand simulations at 230 K and volume corresponding to that of empty hydrate at 20 bar and 230 K. In addition, the water molecules are kept frozen at their initial positions in the constant volume simulations. The figure is similar to Figure 7 from Wierzchowski and Monson.[36] The data plotted in the figure show a close match between the simulation results with frozen water and vdWP theory predictions accounting for all the interactions. This shows that the mean-field approximation is quite appropriate for describing the methane−methane interactions. The original version of the vdWP theory, which only accounts for interactions between methane and water

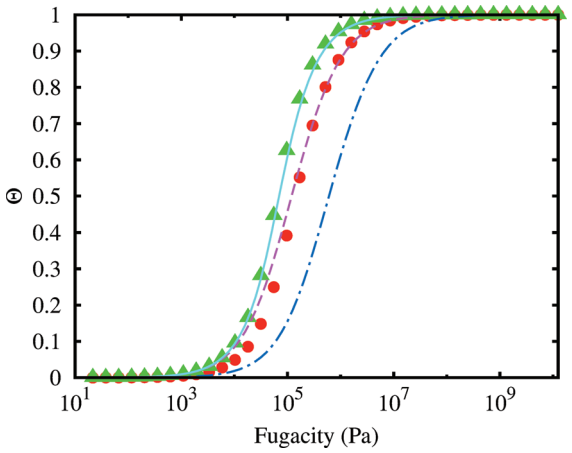

Figure 1. Fractional occupancy of methane in sI hydrate at 230 K and 20 bar. The circles denote results from constant pressure semigrand simulations. The triangles denote results from constant volume semigrand simulations with frozen water. The three lines show the vdWP result with different levels of approximation, namely, (i) neglecting methane−methane interactions and methane−water interactions beyond the first cage (dot-dashed), (ii) neglecting only the methane−methane interactions (dashed), and (iii) including methane−water interactions and methane−methane interactions via eq 7 (solid).

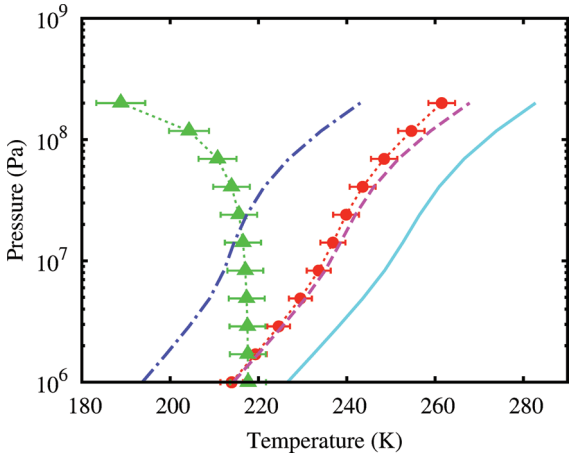

Figure 2. $P-T$ phase diagram for methane sI hydrate. The circles show the equilibria between the liquid, vapor, and hydrate phase obtained from simulations. The predictions from vdWP theory with different levels of approximation are also shown. The approximations used include (i) neglecting methane−methane interactions and methane−water interactions beyond the first cage (dot-dashed line), (ii) neglecting only the methane−methane interactions (dashed line), and (iii) including both the methane−water interactions and methane−methane interactions (solid line). Also shown are the equilibria between liquid water and ice-Ih (triangles) for the SPC/E water model. The dotted lines between the symbols serve as a guide to the eye. The size of the error bars indicates 95% confidence level estimated from five independent simulations.

molecules belonging to the cage surrounding it, underestimates the occupancy for obvious reasons. There is also a significant difference in the occupancy of methane between the constant pressure and constant volume simulations with frozen water molecules. This is because it is much easier to insert methane molecules inside the hydrate framework if the water molecules are kept frozen because the movement of water molecules reduces the net space available inside each cage to insert methane molecules. As concluded by Wierzchowski and Monson,[36] this indicates that it is necessary to account for movement of water molecules in the vdWP theory for accurate prediction of the occupancy of cages even if all the intermolecular interactions are known exactly. Figure 2 shows the triple-point line denoting equilibria between liquid water, methane vapor, and the sI-hydrate phase. Also shown is the equilibrium line between liquid water and ice-Ih. The triple-point lines from the vdWP theory were calculated using eqs 6 and 8 in the following manner. Substituting eq 13 into the aforementioned equations, we can rewrite them as

$$\ln(f_w^l) - \ln(f_w^0) = -\nu_L \ln[1 + f_g C_L] - \nu_S \ln[1 + f_g C_S] \quad (20)$$

$$\ln(f_w^l) - \ln(f_w^0) = -\nu_L \ln[1 + f_g \exp(-\beta\Theta a_L) C_L] - \nu_S \ln[1 + f_g \exp(-\beta\Theta a_S) C_S] \quad (21)$$

respectively. In eqs 20 and 21, the LHSs were calculated using the equations of state obtained from simulations. The value of the fugacity of methane in the RHSs was obtained from the LJ equation of state,[46] and those of ethane were obtained from simulations. Thus, the only approximation involved while applying vdWP theory is in the calculation of the Langmuir constant. The values of a_L and a_S for the methane hydrate were obtained by keeping methane molecules at the centers of the cages in the hydrate phase. In the case of ethane, a_L was obtained by keeping ethane molecules at the centers of the larger tetrakaidecahedron cavities. The orientations of the ethane molecules were obtained after energy minimization. The system size used for calculation of a_L and a_S was equal to the volume of eight unit cells of empty hydrate. As described in Section 2, the methane−water interactions are accurately accounted for via Monte Carlo integration. During the calculation of the Langmuir constant, the length of the unit cell of the hydrate phase was kept equal to 11.81 Å. Figure 1 showed that the use of mean-field approximation for methane−methane interactions is justified. From Figure 2, we observe that if only interactions of methane with water molecules belonging to the cage surrounding it are included the triple-point temperatures are about 20−25 K smaller than the simulations. Accurately including all the methane−water interactions improves the situation quite a bit, and the theoretical predictions are much closer to the exact equilibrium line. However, this is somewhat fortuitous and is a result of cancellation of errors occurring in the vdWP theory.[36] When all the interactions, i.e., methane−water and methane−methane, are properly accounted for within the methane hydrate, the vdWP theory over-estimates the dissociation temperatures by 10−15 K for the pressures studied here.

We now present the results of our study with ethane sI-hydrate and compare it with methane hydrate. This comparison highlights the severity of approximations of the vdWP theory on guests that are nonspherical and larger than methane. Figure 3 shows the occupancy curves for ethane in sI hydrate as a function of its fugacity. The two sets of simulation data were obtained from constant pressure semigrand simulations at 220 K and 7 bar and constant volume semigrand simulations with frozen water at 220 K. The volume of the sI hydrate in the constant volume simulations was kept equal to the volume of the empty sI hydrate at 220 K and 7 bar. Again, similar to methane, we find a close

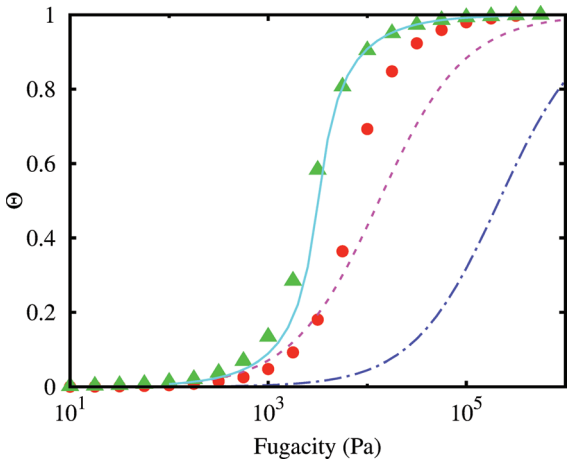

Figure 3. Fractional occupancy of ethane in sI hydrate at 230 K and 20 bar. The circles denote results from constant pressure semigrand simulations. The triangles denote results from constant volume semigrand simulations with frozen water. The three lines show the vdWP result with different levels of approximation, namely (i) neglecting ethane−ethane interactions and ethane−water interactions beyond the first cage (dot-dashed), (ii) neglecting only the ethane−ethane interactions (dashed), and (iii) including ethane−water interactions and ethane−ethane interactions via eq 7 (solid).

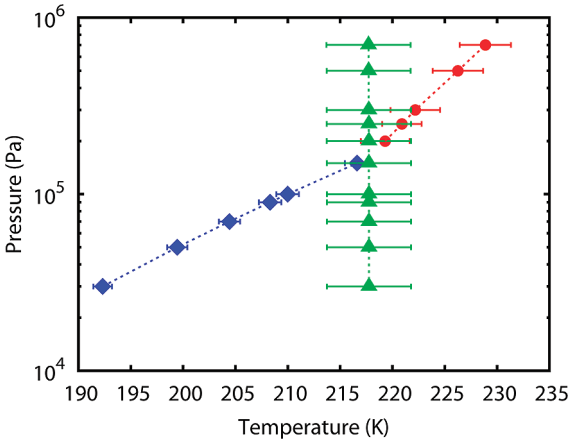

Figure 4. $P-T$ phase diagram for ethane sI hydrate. The circles show the equilibria between the liquid, vapor, and hydrate phase obtained from simulations. The diamonds show the equilibria between the ice-Ih, vapor, and hydrate phase. Also shown are the equilibria between liquid water and ice-Ih (triangles) for the SPC/E water model. The dotted lines between the symbols serve as a guide to the eye. The size of the error bars indicates a 95% confidence level estimated from five independent simulations.

agreement between the simulation results with frozen water and vdWP theory predictions accounting for all the intermolecular interactions. This justifies the use of the mean-field approximation for ethane−ethane interactions. All the conclusions that we infer from Figure 1 are also valid for the ethane hydrate. The disagreement between the simulation results and the vdWP theory predictions that only account for ethane-water interactions are much more severe than methane hydrate. We further observe that the variation of the occupancy of ethane from zero occupancy to full occupancy occurs over a much shorter range of fugacity compared to the vdWP theory predictions that only

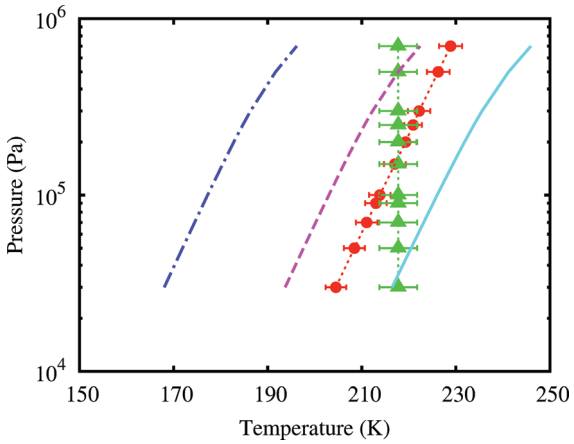

Figure 5. $P-T$ phase diagram for ethane sI hydrate. The circles show the equilibria between the liquid, vapor, and hydrate phase obtained from simulations. The predictions from vdWP theory with different levels of approximation are also shown. The approximations used include (i) neglecting ethane−ethane interactions and ethane−water interactions beyond the first cage (dot-dashed line), (ii) neglecting only the ethane−ethane interactions (dashed line), and (iii) including both the ethane−water interactions and ethane−ethane interactions (solid line). Also shown are the equilibria between liquid water and ice-Ih (triangles) for the SPC/E water model. The dotted lines between the symbols serve as a guide to the eye. The figure shows both the stable and the metastable branches of the triple-point lines obtained from simulations and vdWP theories. The size of the error bars indicates a 95% confidence level estimated from five independent simulations.

account for ethane−water interactions. Only when ethane−ethane interactions are included do the vdWP theory predictions show a similar variation in the occupancy compared to simulations. This indicates the necessity of including guest−guest interactions in the vdWP theory, especially for nonspherical molecules such as ethane. The $P-T$ phase diagram for the ethane hydrate as obtained from simulations is shown in Figure 4. For the ranges of the temperature and pressure considered here, this includes the first quadruple point denoting equilibrium between liquid water, ice-Ih, ethane vapor, and the sI hydrate. Figures 5 and 6 show a comparison between the simulation results and the predictions of the vdWP theory for triple-point lines. For clarity, we have also shown the metastable branches of the equilibrium lines. The disagreement between simulation results and theoretical predictions is much larger than that for methane hydrate. Overall, from our study of methane and ethane hydrates, we can conclude that accurately accounting for the intermolecular interactions is not sufficient, and it is important to include the effect of movement of water molecules in the hydrate phase for accurate prediction of the phase equilibria.

Regarding the effect of noninclusion of guest−guest interactions and interactions of the guest with host molecules beyond the nearest neighbors, our studies show that these interactions contribute significantly to the partition function and thus cannot be ignored. Figures 1 to 3, 5, and 6 clearly show that the predictions of the vdWP theory differ significantly depending upon inclusion or noninclusion of these interactions. The inclusion of these interactions makes the hydrate phase more stable, resulting in a significant increase in the value of dissociation temperature. For the systems studied here, this amounts to an increase of 50 K for methane hydrates and around 70−80 K for ethane hydrates. Surprisingly, the slopes of the triple-point lines

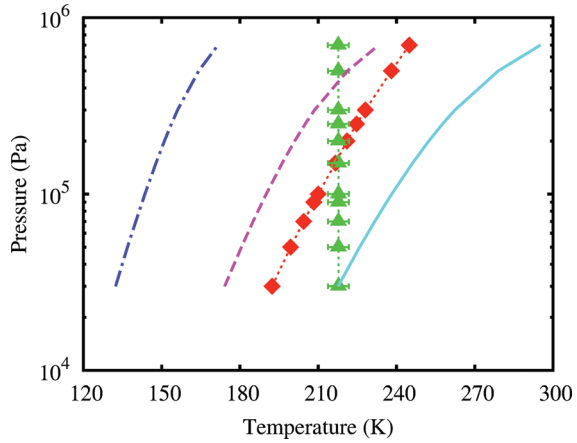

Figure 6. $P-T$ phase diagram for ethane sI hydrate. The diamonds show the equilibria between the ice-Ih, vapor, and hydrate phase obtained from simulations. The predictions from vdWP theory with different levels of approximation are also shown. The approximations used include (i) neglecting ethane−ethane interactions and ethane−water interactions beyond the first cage (dot-dashed line), (ii) neglecting only the ethane−ethane interactions (dashed line), and (iii) including both the ethane−water interactions and ethane−ethane interactions (solid line). Also shown are the equilibria between liquid water and ice-Ih (triangles) for the SPC/E water model. The dotted lines between the symbols serve as a guide to the eye. The figure shows both the stable and the metastable branches of the triple-point lines obtained from simulations and vdWP theories. The size of the error bars indicates a 95% confidence level estimated from five independent simulations.

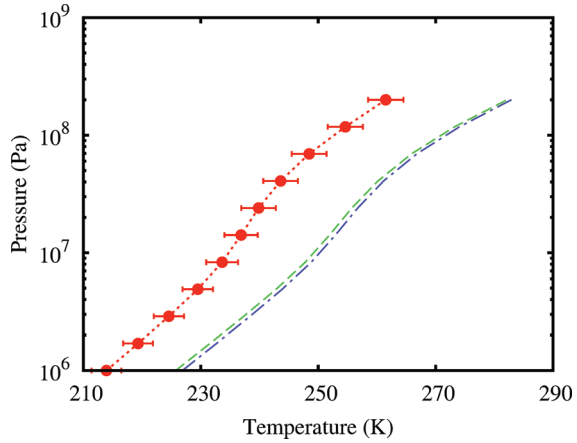

Figure 7. $P-T$ phase diagram for methane sI hydrate. The circles show the equilibria between the liquid, vapor, and hydrate phase obtained from simulations. The dashed and the dot-dashed lines are the vdWP theory prediction taking into account all the intermolecular interactions using the largest and the smallest hydrate volume encountered in our simulations, respectively. The dotted lines between the symbols serve as a guide to the eye. The size of the error bars indicates a 95% confidence level estimated from five independent simulations.

obtained from simulations nearly match those obtained from different versions of the vdWP theory, even though they are different for the occupancy curves. This might explain the relative success of the vdWP theory for modeling gas hydrates even when the intermolecular interactions are not accurately accounted for but are parametrized using the triple-point data. We note that some of the dissociation temperatures predicted from the vdWP

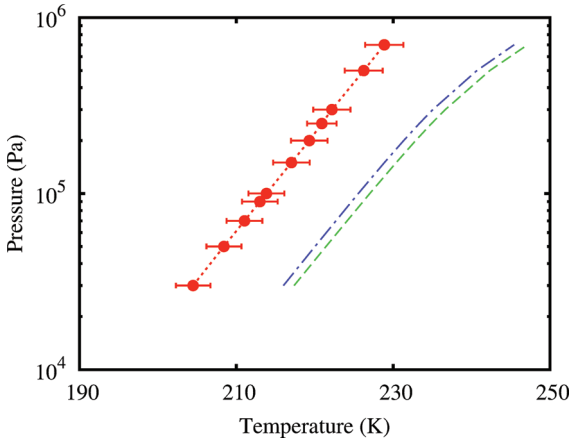

Figure 8. $P-T$ phase diagram for ethane sI hydrate. The circles show the equilibria between the liquid, vapor, and hydrate phase obtained from simulations. The dashed and the dot-dashed lines are the vdWP theory prediction taking into account all the intermolecular interactions using the largest and the smallest hydrate volume encountered in our simulations, respectively. The dotted lines between the symbols serve as a guide to the eye. The size of the error bars indicates a 95% confidence level estimated from five independent simulations.

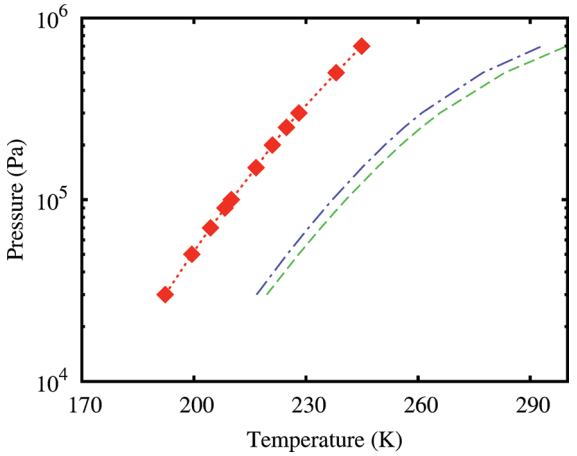

Figure 9. $P-T$ phase diagram for ethane sI hydrate. The diamonds show the equilibria between the ice-Ih, vapor, and hydrate phase obtained from simulations. The dashed and the dot-dashed lines are the vdWP theory prediction taking into account all the intermolecular interactions using the largest and the smallest hydrate volume encountered in our simulations, respectively. The dotted lines between the symbols serve as a guide to the eye. The size of the error bars indicates a 95% confidence level estimated from five independent simulations.

theory are beyond the ranges where simulations were performed. These were obtained by extrapolation of the equations of state of water and empty hydrate. However, since the differences between theory and simulations are nearly uniform across all temperature ranges, the conclusions from our study still remain valid.

Finally, we look at the effect of including volume changes in the hydrate phase on the calculation of the Langmuir constant. Ballard and Sloan[30,31] incorporated the effect of volume changes in the hydrate phase during occupancy of the cages by guest molecules while calculating the fugacity of water. This relaxes, somewhat, the criteria of the rigid water lattice. Ballard and Sloan[30] show that incorporation of volume changes in the

hydrate phase helps them to predict a maximum in the dissociation temperature of methane at high pressures, where the compression of the cages causes methane to no longer fit into the smaller cages. To understand the effect of hydrate volume changes on the phase equilibrium line, we compute the triple points using vdWP theory for the maximum and the minimum hydrate volumes seen in our simulations. These corresponded to unit cells of sizes 11.895 and 11.835 Å, respectively. Comparisons of these predictions are shown in Figures 7−9. The figures clearly show that the incorporation of the volume changes has a very small effect on the phase equilibrium line within the ranges of pressures considered. Thus, we can conclude that relaxation of the assumption of rigid water lattice via incorporation of volume changes does not account for movement of water molecules adequately.

6. CONCLUSIONS

In this study, we have examined the approximation of a rigid water lattice in the theory for gas hydrates. We computed the triple-point lines in methane and ethane hydrates from Monte Carlo simulations and compared them with predictions of vdWP theory. In the application of the vdWP theory, the properties of liquid water, ice-Ih, empty hydrate, and the vapor phase were obtained from the simulations. Thus, the only approximation involved was in the calculation of the Langmuir constant. Our study showed that even if all the intermolecular interactions are known exactly during the calculation of the Langmuir constant, vdWP theory considerably over-estimates the dissociation temperatures of gas hydrates. The primary reason for this overestimation is the assumption of a rigid water lattice within the vdWP theory. The rigidity of the water lattice makes it easier to accommodate the hydrocarbon guest molecules within the cages of the hydrate phase. This in turn imparts a higher stability to the gas hydrate resulting in the higher dissociation temperatures. Thus, we can conclude that it is necessary to account for the movement of water molecules in the hydrate phase in the development of more robust theories for gas hydrates. Our study also concludes that the guest−guest interactions and guest−host interactions beyond the nearest-neighbor interactions contribute significantly to the partition function and cannot be ignored in the theories for gas hydrates.

A. FUGACITY OF WATER IN THE HYDRATE PHASE IN EQUILIBRIUM WITH THE VAPOR PHASE

In this section, we derive an expression for the fugacity of water in the hydrate phase that is in equilibrium with the hydrocarbon vapor phase. The starting point is the Gibbs−Duhem equations for the hydrate and the vapor phases, respectively.

$$x_w^H d\ln f_w^H + x_g^H d\ln f_g^H = H_R^H d\left(\frac{1}{RT^H}\right) + Z^H d\ln P^H \quad (22)$$

$$d\ln f_g^v = H_R^v d\left(\frac{1}{RT^v}\right) + Z^v d\ln P^v \quad (23)$$

Through the application of phase equilibria criteria (eqs 9, 10, and 14), f_g can be eliminated resulting in the following equation.

$$x_w^H d\ln f_w^H = (H_R^H - x_g^H H_R^v) d\left(\frac{1}{RT}\right) + (Z^H - x_g^H Z^v) d\ln P \quad (24)$$

where we have dropped the superscripts for T and P. Integrating the above equation we get

$$\ln\left(\frac{f_w^H}{f_{w,0}^H}\right) = \int_{T_0}^{T}\left(\frac{H_R^H - x_g^H H_R^v}{x_w^H}\right)_P d\left(\frac{1}{RT}\right) + \int_{P_0}^{P}\left(\frac{Z^H - x_g^H Z^v}{x_w^H}\right)_{T_0} d\ln P \quad (25)$$

ASSOCIATED CONTENT

Supporting Information. Equations of state for liquid water, ice-Ih, and empty hydrate phases. This material is available free of charge via the Internet at http://pubs.acs.org.

AUTHOR INFORMATION

Corresponding Author
*E-mail: sudeep@chemeng.iisc.ernet.in.

REFERENCES

(1) Sloan, E. D.; Koh, C. A. *Clathrate Hydrates of Natural Gases*, 3rd ed.; CRC Press: Boca Raton, FL, 2007.
(2) Sloan, E. D. *Nature* **2003**, *426*, 353–359.
(3) Hammerschmidt, E. G. *Ind. Eng. Chem.* **1934**, *26*, 851–855.
(4) Vysniauskas, A.; Bishnoi, P. R. *Chem. Eng. Sci.* **1983**, *38*, 1061–1972.
(5) Bishnoi, P. R.; Natarajan, V. *Fluid Phase Equilib.* **1996**, *117*, 168–177.
(6) Walsh, M. R.; Koh, C. A.; Sloan, E. D.; Sum, A. K.; Wu, D. T. *Science* **2009**, *326*, 1095–1098.
(7) Sloan, E. D. *Fluid Phase Equilib.* **2005**, *228−229*, 67–74.
(8) Gudmundsson, J.; Borrehaug, A. *Proc. 2nd Int. Conf. Nat. Gas Hydrates* **1996**, 415–422.
(9) Khokhar, A. A.; Gudmundsson, J.; Sloan, E. D. *Fluid Phase Equilib.* **1998**, *150−151*, 383–392.
(10) Englezos, P. *Ind. Eng. Chem. Res.* **1993**, *32*, 1251–1274.
(11) Linga, P.; Kumar, R.; Englezos, P. *J. Hazard. Mater.* **2007**, *149*, 625–629.
(12) Dickens, G. R. *Earth Planet Sci. Lett.* **2003**, *213*, 169–183.
(13) van der Waals, J. H.; Platteeuw, J. C. *Adv. Chem. Phys.* **1959**, *2*, 1–57.
(14) Lennard-Jones, J. E.; Devonshire, A. F. *Proc. R. Soc. London* **1937**, *163*, 53–70.
(15) Lennard-Jones, J. E.; Devonshire, A. F. *Proc. R. Soc. London* **1938**, *165*, 1–11.
(16) McKoy, V.; Sinanoglu, O. *J. Chem. Phys.* **1963**, *38*, 2946–2956.
(17) John, V. T.; Holder, G. D. *J. Phys. Chem.* **1981**, *85*, 1811–1814.
(18) John, V. T.; Holder, G. D. *J. Phys. Chem.* **1982**, *86*, 455–459.
(19) John, V. T.; Holder, G. D. *J. Phys. Chem.* **1985**, *89*, 3279–3285.
(20) Sparks, K. A.; Tester, J. W. *J. Phys. Chem.* **1992**, *96*, 11022–11029.
(21) Sparks, K. A.; Tester, J. W.; Cao, Z.; Trout, B. L. *J. Phys. Chem. B* **1999**, *103*, 6300–6308.
(22) Cao, Z.; Tester, J. W.; Sparks, K. A.; Trout, B. L. *J. Phys. Chem. B* **2001**, *105*, 10950–10960.
(23) Anderson, B. J.; Tester, J. W.; Trout, B. L. *J. Phys. Chem. B* **2004**, *108*, 18705–18715.
(24) Anderson, B. J.; Bazant, M. Z.; Tester, J. W.; Trout, B. L. *J. Phys. Chem. B* **2005**, *109*, 8153–8163.
(25) Klauda, J. B.; Sandler, S. I. *Ind. Eng. Chem. Res.* **2000**, *39*, 3377–3386.
(26) Klauda, J. B.; Sandler, S. I. *J. Phys. Chem. B* **2002**, *106*, 5722–5732.
(27) Bazant, M. Z.; Trout, B. L. *Phys. A* **2001**, *300*, 139–173.
(28) Tanaka, H.; Nakatsuka, T.; Koga, K. *J. Chem. Phys.* **2004**, *121*, 5488–5493.

(29) Klauda, J. B.; Sandler, S. I. *Chem. Eng. Sci.* **2003**, *58*, 27–41.
(30) Ballard, A. L.; Sloan, E. D. *Fluid Phase Equilib.* **2002**, *194*, 371–383.
(31) Ballard, A. L.; Sloan, E. D. *J. Supramol. Chem.* **2002**, *2*, 385–392.
(32) Chialvo, A. A.; Houssa, M.; Cummings, P. T. *J. Phys. Chem. B* **2002**, *106*, 442–451.
(33) Rodger, P. M. *J. Phys. Chem.* **1990**, *94*, 6080–6089.
(34) Rodger, P. M. *AIChE J.* **1991**, *37*, 1511–1516.
(35) Sizov, V. V.; Piotrovskaya, E. M. *J. Phys. Chem. B* **2007**, *111*, 2886–2890.
(36) Wierzchowski, S. J.; Monson, P. A. *J. Phys. Chem. B* **2007**, *111*, 7274–7282.
(37) Wierzchowski, S. J.; Monson, P. A. *Ind. Eng. Chem. Res.* **2006**, *45*, 424–431.
(38) Jensen, L.; Thomsen, K.; van Solms, N.; Wierzchowski, S. J.; Walsh, M. R.; Koh, C. A.; Sloan, E. D.; Wu, D. T.; Sum, A. K. *J. Phys. Chem. B* **2010**, *114*, 5775–5782.
(39) Conde, M. M.; Vega, C. *J. Chem. Phys.* **2010**, *133*, 064507.
(40) Martin, M. G.; Siepmann, J. I. *J. Phys. Chem. B* **1998**, *102*, 2569–2577.
(41) Berendsen, H. J. C.; Grigera, J. R.; Straatsma, T. P. *J. Phys. Chem.* **1987**, *91*, 6269–6271.
(42) Errington, J. R.; Boulougouris, G. C.; Economou, I. G.; Panagiotopoulos, A. Z.; Theodorou, D. N. *J. Phys. Chem. B* **1998**, *102*, 8865–8873.
(43) Vega, C.; Sanz, E.; Abascal, J. L. F.; Noya, E. G. *J. Phys.: Condens. Matter* **2008**, *20*, 153101.
(44) Frenkel, D.; Ladd, A. J. C. *J. Chem. Phys.* **1984**, *81*, 3188–3193.
(45) Polson, J. M.; Trizac, E.; Pronk, S.; Frenkel, D. *J. Chem. Phys.* **2000**, *112*, 5339–5342.
(46) Johnson, J. K.; Zollweg, J. A.; Gubbins, K. E. *Mol. Phys.* **1993**, *78*, 591–618.